A Spatial Mechanism for the Measurement of the Inertia Tensor: Theory and Experimental Results

M. Da Lio

A. Doria

R. Lot

Department of Mechanical Engineering,
University of Padova,
35131 Padova, Italy
E-MAIL: doria@dim.unipd.it

This paper deals with the problem of measuring the inertia tensor of rigid bodies. An original approach is adopted, different from classical modal analysis techniques. The rigid body is forced by a spatial mechanism to rotate around different axes. Once the mechanism is calibrated, i.e., its inertia and stiffness matrices are known, the inertia tensor of the rigid body may be determined by measuring the frequencies of the small oscillations around the selected axes and then solving a least-squares identification problem. Two prototypes of the spatial mechanism were built. The first was used to perform tests and to measure the inertia tensor of some compressors for domestic refrigeration. The second was constructed to measure the inertia tensor of large mechanical systems.

1 Introduction

The dynamic simulation of a mechanical system often requires accurate knowledge of the inertia properties of the rigid bodies which form it. The need for precise evaluation of the inertia tensor is particularly important in the simulation of the dynamics of aircraft and spacecraft (Buyanov, 1991), vehicles (Durisek et al., 1997; Cossalter et al., 1998), robots and automated processes (Gentile et al., 1995).

During the last few decades, several new methods for determining rigid-body inertia properties have been proposed, because the traditional trifilar pendulum tests are time-consuming if precise results are needed, and difficult or expensive when large bodies (like vehicles) are considered.

Several methods are based on Frequency Response Functions (FRF) which are measured during vibrations having six degrees of freedom (Toivola and Nuutila, 1993; Fregolent et al., 1992; Pandit et al., 1992).

The Modal Model Method (MMM) uses orthogonality conditions to determine the mass matrix from the modal model and requires at least six measurement points. The Inertia Restraint Method (IRM) is based on rigid-body residual inertia which is calculated from the measured FRF and also requires at least six response locations. The Direct System Identification Method (DSIM) is based on minimization of the error between measured and theoretical rigid-body FRF, and again needs at least six response locations. Pandit and Hu (1994) recently proposed a method which yields some improved accuracy in the determination of mass matrix and especially in estimation of the center of mass location.

Other authors have proposed measurement methods which make use of equipment which allows the rigid body to rotate only around a fixed axis (Durisek et al., 1997; Gentile et al., 1995). Calculation of the moments and products of inertia with respect to the axis of rotation is carried out on the basis of reaction forces exerted on the shaft by a bearing. The rigid body must be located on the equipment at various orientations in order to measure the whole inertia tensor.

In this paper, a new method for measuring of the inertia tensor is proposed. Measurement is carried out by means of a spatial mechanism which allows the rigid body to rotate around an axis each time. The direction of this axis may be modified by adjusting the positions of two fixed pivots without moving the rigid body. Free damped oscillations around the selected axis occur thanks to an elastic suspension system. The moment of inertia with respect to the selected rotation axis is then calculated by measuring the natural frequency of the oscillation around that axis. In order to determine the inertia tensor of the body, the direction of the axis of rotation is modified several times and the corresponding moments of inertia are calculated; the elements of the tensor are then identified by solving a least-squares problem.

The proposed mechanism is a sort of "weighing machine" which measures the tensor of inertia of a body about a given point, and is suitable for routine measurements.

Since only the free oscillations of the system are considered, the use of shakers and knowledge of forces are not required. In addition, only one acceleration measurement at any time is necessary, compared to the six (at least) simultaneous measurements required by the above-mentioned methods.

Two spatial mechanisms for measuring of the inertia tensor were built and tested. The first is a small device suitable for measuring of the inertia tensor of small specimens (maximum dimension 250 mm, maximum mass 6 kg). The second is larger (mass range 50 ÷ 200 kg, maximum length about 2 m).

This paper presents the kinematic and dynamic analyses of the spatial mechanism for measuring the inertia tensor, and describes the principle of identification and calibration procedures. Some examples of inertia tensor identification are then given and discussed.

2 Kinematic Analysis

Figure 1 shows the spatial mechanism for measuring the inertia tensor; Fig. 2 is a photograph of the smaller version of the prototype mechanism. A fixed coordinate system XYZ with origin at point O is introduced; axis Z is vertical, whereas axes X and Y lie in the horizontal plane.

Plate π, which is used to mount the specimen, rotates around fixed point O, where there is a spherical pair. This pair is air-lubricated in order to reduce friction torque.

Disks C_1 and C_2 rotate around axes X and Y, respectively, by means of two revolute joints and are named "adjustment disks." Connecting rods AA′ and BB′ join two points of the

Contributed by the Dynamic Systems and Control Division for publication in the JOURNAL OF DYNAMIC SYSTEMS, MEASUREMENT, AND CONTROL. Manuscript received by the Dynamic Systems and Control Division April 29, 1998. Associate Technical Editor: T. Kurfess.

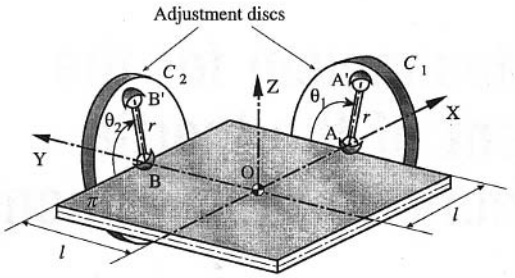

Fig. 1 Diagram of spatial mechanism for measuring inertia tensor

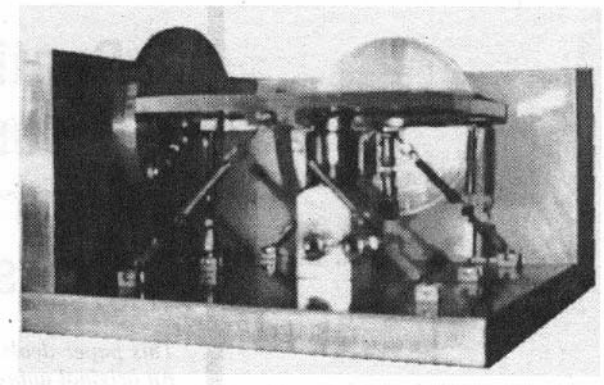

Fig. 2 Prototype of spatial mechanism for measuring inertia tensor

two perpendicular edges of the plate (A and B) with two points of adjustment disks A′, B′. There are spherical pairs in A, B, A′, and B′. The mechanism has five degrees of freedom; two are associated with rotations θ_1 and θ_2 of the adjustment disks. When the rotations of the disks are locked, points A′ and B′ are fixed and the plate with its connecting rods makes up a spatial mechanism having three degrees of freedom. One degree of freedom is associated with the rotation of the plate around an axis passing through point O, direction of which generally changes with the configuration of the mechanism. The other two degrees of freedom are the rotations of the connecting rods around their axes, which do not influence plate motion.

If only small oscillations are considered, the axis of rotation of the plate does not change its direction significantly. Hence, by means of the spatial mechanism, the specimen rotates around a fixed axis the direction of which is determined by setting rotations θ_1 and θ_2.

2.1 Direction of Rotation Axis. The first kinematic problem is determination of the plate rotation axis as a function of θ_1 and θ_2, which is solved following the Gupta method (1973), as shown below.

First the following equations, which specify constant lengths for connecting rods AA′ and BB′, are considered:

$$(A_x - A'_x)^2 + (A_y - A'_y)^2 + (A_z - A'_z)^2 = (A_{x0} - A'_x)^2 + (A_{y0} - A'_y)^2 + (A_{z0} - A'_z)^2 \quad (1)$$

$$(B_x - B'_x)^2 + (B_y - B'_y)^2 + (B_z - B'_z)^2 = (B_{x0} - B'_x)^2 + (B_{y0} - B'_y)^2 + (B_{z0} - B'_z)^2 \quad (2)$$

where A_{x0}, A_{y0}, A_{z0}, B_{x0}, B_{y0}, B_{z0} are the initial coordinates of points A and B, A_x, A_y, A_z, B_x, B_y, B_z are the final coordinates of points A and B, and A'_x, A'_y, A'_z, B'_x, B'_y, B'_z are the coordinates of points A′ and B′. The system is symmetric and the plate in the initial configuration is parallel to the XY plane, hence: $A_{x0} = l$, $A_{y0} = 0$, $A_{z0} = 0$, $B_{x0} = 0$, $B_{y0} = l$, $B_{z0} = 0$, $A'_x = l$, $B'_y = l$, where l is half-width of plate.

The final coordinates of points A and B may be calculated by means of the rotation matrix $[R_{\varphi u}]$ of the plate:

$$\begin{Bmatrix} A_x \\ A_y \\ A_z \end{Bmatrix} = [R_{\varphi u}] \begin{Bmatrix} l \\ 0 \\ 0 \end{Bmatrix} \quad \begin{Bmatrix} B_x \\ B_y \\ B_z \end{Bmatrix} = [R_{\varphi u}] \begin{Bmatrix} 0 \\ l \\ 0 \end{Bmatrix} \quad (3)$$

As plate motion is assumed to be a small rotation φ around an axis passing through point O, the rotation matrix may be written as:

$$[R_{\varphi u}] = \begin{bmatrix} 1 & -u_z\varphi & u_y\varphi \\ u_z\varphi & 1 & -u_x\varphi \\ -u_y\varphi & u_x\varphi & 1 \end{bmatrix} \quad (4)$$

where u_x, u_y, u_z are the unknown components of unit vector u of the rotation axis, which satisfy the condition of unit length:

$$u_x^2 + u_y^2 + u_z^2 = 1 \quad (5)$$

The components of the unit vector of the rotation axis are

Nomenclature

A_{x0}, A_{y0}, A_{z0} = initial coordinates of point A
A_x, A_y, A_z = final coordinates of point A
A'_x, A'_y, A'_z = coordinates of points A′
B_{x0}, B_{y0}, B_{z0} = initial coordinates of point B
B_x, B_y, B_z = final coordinates of point B
B'_x, B'_y, B'_z = coordinates of points B′
a_i = dimension of inertia ellipsoid in direction $\mathbf{u}_i$
c_u = damping around axis $\mathbf{u}$
f = regression degrees of freedom
g = gravity acceleration
$[I_o]$ = inertia tensor relative to point O
$[I_{op}]$ = plate inertia tensor
$[I_{os}]$ = specimen inertia tensor
I_u = inertia moment relative to axis $\mathbf{u}$
$[J]$ = Jacobian matrix
$[k_o]$ = stiffness matrix relative to point O
$[k_{op}]$ = plate stiffness matrix
$[k_{os}]$ = specimen stiffness matrix
k_u = stiffness around axis $\mathbf{u}$
l = half-width of plate
m_s = mass of specimen
m_p = mass of plate
m = number of measurements for calibration
n = number of measurements for identification
q = natural frequency of damped vibrations
r = connecting rod length
$[R_{\varphi u}]$ = rotation matrix around axis $\mathbf{u}$
s_1 s_2 = singular values of Jacobian matrix
$\mathbf{u}$ = unit vector of rotation axis
x_p, y_p, z_p = coordinates of plate center of mass
x_s, y_s, z_s = coordinates of specimen center of mass
xyz = body coordinate system
XYZ = fixed coordinate system
ϵ_i = residual
θ_1, θ_2 = rotations of adjustment disks
ζ = damping ratio
$\hat{\sigma}_1$ = root mean square of residuals
τ_u = constant gravity torque
φ = plate rotation
ω_n = natural frequency

Superscript

T = transposition

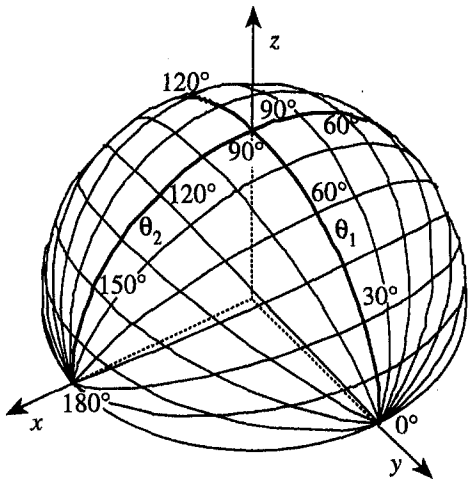

Fig. 3 Direction of rotation axis as a function of θ_1 and θ_2

found by substituting Eqs. (3) and (4) into Eqs. (1) and (2) and solving (1), (2), (5) together. Since only small rotations φ are considered, the unit vector components depend on the coordinates of points A′ and B′ only (otherwise they also would depend on φ). The coordinates of points A′ and B′ on the adjustment disks are expressed in terms of the rotations of the disks by equations:

$$A'_y = r\cos\theta_1 \quad A'_z = r\sin\theta_1$$
$$B'_x = -r\cos\theta_2 \quad B'_z = r\sin\theta_2 \tag{6}$$

where r is the length of the connecting rods.

The final formulas, which give the components of the unit vector of the rotation axis, are:

$$u_x = -\frac{\cos(\theta_2)\sin(\theta_1)}{\sqrt{1-\cos^2(\theta_2)\cos^2(\theta_1)}},$$
$$u_y = \frac{\cos(\theta_1)\sin(\theta_2)}{\sqrt{1-\cos^2(\theta_2)\cos^2(\theta_1)}},$$
$$u_z = \frac{\sin(\theta_2)\sin(\theta_1)}{\sqrt{1-\cos^2(\theta_2)\cos^2(\theta_1)}} \tag{7}$$

and hold for small rotations only.

Figure 3 shows how the direction of the rotation axis depends on θ_1 and θ_2.

2.2 Accuracy of Direction of Rotation Axis. Even when small rotations are considered, the direction of the rotation axis may deviate from that defined by Eqs. (7). This may happen if the plate oscillates from an initial configuration which does not exactly coincide with plane XY (owing to unbalanced mass, as will be shown below) or if there are errors in the dimensions of the links and values of θ_1 and θ_2 (adjustment errors). The first cause of deviation may be reduced by accurate alignment of the plate to the horizontal plane. Dimensional errors may be minimized by careful construction.

If the configuration defined by θ_1 and θ_2 is close to a singular configuration of the mechanism, adjustment errors will be amplified, causing large deviations of the rotation axis. Therefore, precise measurements can be carried out only far from a singular configuration. In order to study this important problem, Eqs. (7) are differentiated, yielding the following set of linear equations:

$$\begin{Bmatrix} du_x \\ du_y \\ du_z \end{Bmatrix} = [J]\begin{Bmatrix} d\theta_1 \\ d\theta_2 \end{Bmatrix} \tag{8}$$

Transformation (8) maps a circle in the space of adjustment errors into an ellipse in the space of orientation errors. The singular values of the Jacobian matrix $[J]$ are the lengths of the axes of the ellipse which corresponds to a circle of unit radius. If adjustment errors are assumed to belong to a small circular neighborhood of radius δ, the maximum orientation error is $s_1\delta$ and the minimum orientation error is $s_2\delta$, where s_1 and s_2 are the maximum and minimum singular values, respectively. Therefore, the maximum singular value is an index of the error amplification caused by the kinematics of the mechanism. For the above Jacobian matrix, this value is:

$$s_1 = \sqrt{\frac{1}{\sin^2(\theta_2) + \cos^2(\theta_2)\sin^2(\theta_1)}} \tag{9}$$

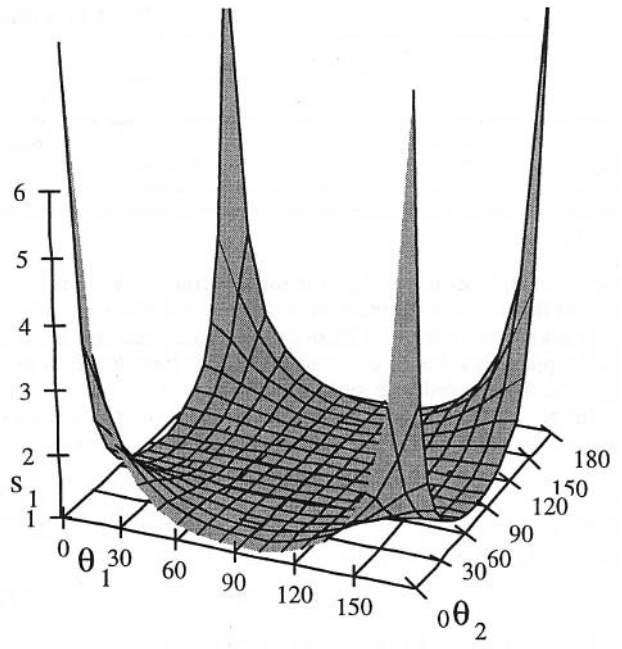

Fig. 4 Maximum singular value of Jacobian matrix as a function of θ_1 and θ_2

Figure 4 shows the maximum singular value as a function of θ_1 and θ_2, and highlights the fact that there is no kinematic amplification of errors when the rotation axis overlaps axes X, Y, and Z, and that kinematic amplification is very large only when both connecting rods tend to lie on the horizontal plane.

3 Dynamic Analysis

Once the axis of rotation (represented by unit vector $\mathbf{u}$) has been fixed by setting θ_1 and θ_2, the equation of the small oscillation of the system is the following:

$$I_u\ddot{\varphi} + c_u\dot{\varphi} + k_u\varphi = \tau_u \tag{10}$$

where I_u is the mass moment of inertia relative to axis $\mathbf{u}$, c_u is

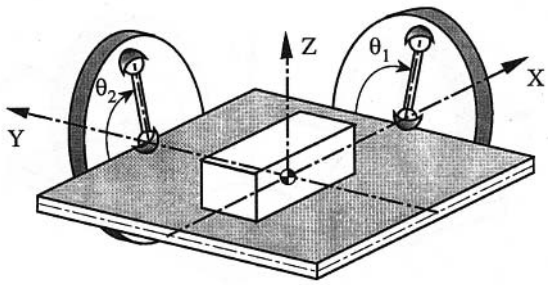

Fig. 5 Measurement of inertia tensor of first block

Table 1 Results of first identification test ($\hat{\sigma}_1 = 0.00006$ kgm^2)

	Inertia moments [kgm^2]			Inertia products [kgm^2]			Principal moments [kgm^2]		
	I_{xx_o}	I_{yy_o}	I_{zz_o}	I_{xy_o}	I_{xz_o}	I_{yz_o}	I_1	I_2	I_3
Analytic	0.00247	0.00466	0.00265	0.00000	−0.00005	0.00013	0.00246	0.00266	0.00467
Identified	0.00247	0.00467	0.00263	0.00001	−0.00011	0.00014	0.00241	0.00268	0.00468
Error	—	0.00001	−0.00002	0.00001	−0.00006	0.00001	−0.00005	0.00002	0.00001

the damping coefficient, k_u is torsional stiffness, and τ_u is torque due to the unbalanced mass of specimen and plate.

A coordinate system with origin at O and axes xyz attached to the plate (and hence to the specimen) is introduced; it overlaps the XYZ coordinate system when $\varphi = 0$.

Inertia moment I_u is expressed in terms of inertia tensor $[I_o]$ relative to point O and axes xyz in the following way:

$$I_u = \mathbf{u}^T[I_o]\mathbf{u} \tag{11}$$

In the same manner, stiffness k_u is expressed in terms of stiffness matrix $[k_o]$ relative to point O:

$$k_u = \mathbf{u}^T[k_o]\mathbf{u} \tag{12}$$

The inertia tensor is the sum of two terms:

$$[I_o] = [I_{op}] + [I_{os}] = \begin{bmatrix} I_{xx_{op}} & -I_{xy_{op}} & -I_{xz_{op}} \\ -I_{xy_{op}} & I_{yy_{op}} & -I_{yz_{op}} \\ -I_{xz_{op}} & -I_{yz_{op}} & I_{zz_{op}} \end{bmatrix} + \begin{bmatrix} I_{xx_{os}} & -I_{xy_{os}} & -I_{xz_{os}} \\ -I_{xy_{os}} & I_{yy_{os}} & -I_{yz_{os}} \\ -I_{xz_{os}} & -I_{yz_{os}} & I_{zz_{os}} \end{bmatrix} \tag{13}$$

where the first term is the inertia tensor of the plate (index p) and the second term the unknown inertia tensor of the specimen (index s), both about point O.

The stiffness matrix is also the sum of two terms:

$$[k_o] = [k_{op}] + [k_{os}] \tag{14}$$

The first term $[k_{op}]$ is due to the elastic torques exerted by the suspension system and to position-dependent gravity torque, which is present when the plate oscillates if the center of mass of the plate does not coincide with point O:

$$[k_{op}] = \begin{bmatrix} k_{xx_p} & k_{xy_p} & k_{xz_p} \\ k_{xy_p} & k_{yy_p} & k_{yz_p} \\ k_{xz_p} & k_{yz_p} & k_{zz_p} \end{bmatrix} + gm_p \begin{bmatrix} -z_p & 0 & x_p \\ 0 & -z_p & y_p \\ x_p & y_p & 0 \end{bmatrix} \tag{15}$$

where m_p is the mass of the plate, g the acceleration due to gravity, and x_p, y_p, z_p the coordinates of the plate center of mass.

The second term $[k_{os}]$ takes into account the position-dependent gravity torque which is present when the plate oscillates if the center of mass of the specimen does not coincide with point O:

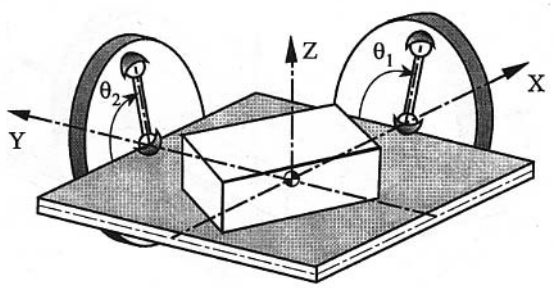

Fig. 6 Measurement of inertia tensor of second block

$$[k_{os}] = gm_s \begin{bmatrix} -z_s & 0 & x_s \\ 0 & -z_s & y_s \\ x_s & y_s & 0 \end{bmatrix} \tag{16}$$

where m_s is the mass of the specimen and x_s, y_s, z_s are the coordinates of the specimen center of mass.

Torque τ_u is a constant gravity torque which is present if the plate and specimen center of mass is not over point O:

$$\tau_u = g(m_s x_s + m_p x_p)u_y - g(m_s y_s + m_p y_p)u_x \tag{17}$$

It modifies the equilibrium position and must be reduced in order to improve measurement precision.

The solution of Eq. (10) is:

$$\varphi(t) = \frac{\tau_u}{k_u} + Ae^{-\zeta\omega_n t}\cos(qt + \psi) \tag{18}$$

where A and ψ are constants, and:

$$\omega_n = \sqrt{k_u/I_u}\,, \quad \zeta = \frac{c_u}{2\sqrt{k_u I_u}}\,, \quad q = \omega_n\sqrt{1-\zeta^2} \tag{19}$$

4 Identification Procedure

Identification of the inertia tensor is carried out with respect to origin O of the plate, the mass of the specimen and its center of mass position are measured before. Frequency q_i and damping ratio ζ_i of the oscillation around arbitrary axis $\mathbf{u}_i$ may easily be measured by means of an accelerometer and a Fourier analyzer (or an oscilloscope); natural frequency ω_{n_i} is then calculated.

Conversely, ω_{n_i} is related to the dynamic properties of the system by the equation:

$$\omega_{n_i}^2 = \frac{k_{u_i}}{I_{u_i}} = \frac{\mathbf{u}_i^T[[k_{op}] + [k_{os}]]\mathbf{u}_i}{\mathbf{u}_i^T[[I_{op}] + [I_{os}]]\mathbf{u}_i} \tag{20}$$

The right-hand term of Eq. (20) depends only on the six elements of the inertia tensor of the specimen $[I_{os}]$, when the inertia tensor of the plate $[I_{op}]$ and the stiffness matrices $[k_{op}]$, $[k_{os}]$ are known. Therefore, if n different orientations of the rotation axis are considered ($i = 1, n$) and the corresponding natural frequencies are measured, a set of n simultaneous equations like Eq. (20) is obtained.

The unknowns of these equations are the six components of the inertia tensor of the specimen with respect to point O and body axes xyz. They are calculated with least-squares approach, and residuals are defined in the following way:

$$\epsilon_i = \mathbf{u}_i^T[[I_{op}] + [I_{os}]]\mathbf{u}_i - \frac{1}{\omega_{n_i}^2}\mathbf{u}_i^T[[k_{op}] + [k_{os}]]\mathbf{u}_i \tag{21}$$

It is worth noting that measured natural frequency ω_{ni} relative to given rotation axis $\mathbf{u}_i$ is proportional to dimension a_i of the inertia ellipsoid in direction $\mathbf{u}_i$:

Table 2 Results of second identification test ($\hat{\sigma}_1 = 0.0005$ kgm^2)

	Inertia moments [kgm^2]			Inertia products [kgm^2]			Principal moments [kgm^2]		
	I_{xx_o}	I_{yy_o}	I_{zz_o}	I_{xy_o}	I_{xz_o}	I_{yz_o}	I_1	I_2	I_3
Analytic	0.02785	0.02810	0.02713	−0.01161	0.00179	−0.00028	0.01617	0.02724	0.03968
Identified	0.02619	0.02847	0.02774	−0.01104	+0.00129	0.00017	0.01617	0.02771	0.03852
Error	−0.00166	0.00037	0.00061	0.00057	−0.00050	0.00045	—	0.00047	−0.00116

$$a_i = \frac{1}{\sqrt{I_{u_i}}} = \frac{\omega_{n_i}}{\sqrt{k_{u_i}}} \tag{22}$$

Hence, to find the whole ellipsoid, it is necessary to span the three-dimensional space with directions $\mathbf{u}_i$.

Once the inertia tensor is identified, the moments of inertia I_{u_i} with respect to the axes which have been used in the measurements can be calculated. The residual root mean square is given by:

$$\hat{\sigma}_1 = \sqrt{\frac{\Sigma_{i=1}^{n} \epsilon_i^2}{n - f - 1}} \tag{23}$$

where $f = 6$ is the number of regression degrees of freedom. Residuals ϵ_i are calculated by substituting identified inertia tensor $[I_{os}]$ into Eq. (21). If systematic errors (like dimensional errors and those caused by the orientation of the axis near the singular configurations of the mechanism) are avoided, $\hat{\sigma}_1$ is a good estimate of the error of the method.

5 Calibration

The identification method requires previous knowledge of matrices $[I_{op}]$ and $[k_{op}]$ of the plate and of matrix $[k_{os}]$ of the specimen. The elements of the last matrix can be calculated separately by measuring the coordinates of the center of mass of the specimen. The inertia and stiffness matrices of the mechanism may be calculated using an identification approach similar to that of the previous section.

A set of rigid bodies, whose inertia properties are known, is necessary. The first rigid body is placed on the mechanism and natural frequencies are measured for several different orientations of rotation axis $\mathbf{u}$. The procedure is repeated for the other rigid bodies. If a total of m measurements are carried out, the following equations hold:

$$\omega_{n_j}^2 = \frac{\mathbf{u}_j^T[[k_{op}] + [k_{os}]]\mathbf{u}_j}{\mathbf{u}_j^T[[I_{op}] + [I_{os}]]\mathbf{u}_j} \quad j = 1, m \tag{24}$$

They have the same form as Eqs. (20), but now the inertia and stiffness matrices of the specimen are known, whereas those of the mechanism are unknown. Therefore, m simultaneous equations in the twelve unknown elements of the inertia and stiffness matrices of the mechanism are obtained. The least-squares method is used to solve this set of equations.

6 Experimental Results

To assess the accuracy of the proposed method, some tests were carried out in which the inertia tensor of simple rigid bodies was measured, thus allowing comparison between analytical and experimental results. The smaller of the two working mechanisms, shown in Fig. 2, was used.

In the first test a parallelepiped block of mass 1.649 kg was located on the plate with its sides parallel to the fixed axes (see Fig. 5). The coordinates of the center of mass were $x_s = -0.95$ mm $y_s = 2.2$ mm $z_s = 35$ mm. Body axes xyz were not exactly the principal axes of inertia relative to point O, because small inertia products were caused by the offset of the center of mass from point O. Nineteen different orientations of the rotation axis were selected and the corresponding natural frequencies were measured. The identified values of the inertia tensor elements are listed in Table 1.

The errors were lower than $\hat{\sigma}_1$ and hence were much smaller than the values of the inertia moments, but comparable to those of the inertia products. The errors in the elements of the inertia tensor may be evaluated by taking into account the fact that the inertia tensor describes the inertia ellipsoid which, with respect to the selected body axes, is invariant. Many dynamic properties of a rigid body (e.g., kinetic energy) are related to the dimensions of the inertia ellipsoid, which are inversely proportional to the square roots of the principal moments of inertia. The values of the principal moments of inertia of the first specimen were then calculated from the identified tensor and compared with the analytical values. The last column of table 1 shows that the dimensions of the inertia ellipsoid were identified with good accuracy, in spite of errors in the values of the inertia products.

In the second test a parallelepiped block of mass 6.2 kg was located on the plate in a tilted position (see Fig. 6). The center of mass coordinates were $x_s = 6.43$ mm, $y_s = -1$ mm, $z_s = 45$ mm. In this position the block had a large product of inertia I_{xy}.

The results of identification are listed in Table 2. The inertia moments and product of inertia I_{xy} were identified with good accuracy. The increase in specimen mass caused larger friction forces and altered the behavior of the air-lubricated bearing,

Table 3 Comparison with other identification methods

	Conti and Bretl	Pandit and Hu	Proposed method 2nd test
I_{xx}%	0.5	13.0	5.9
I_{yy}%	3.0	5.9	1.3
I_{zz}%	18.0	3.8	2.2

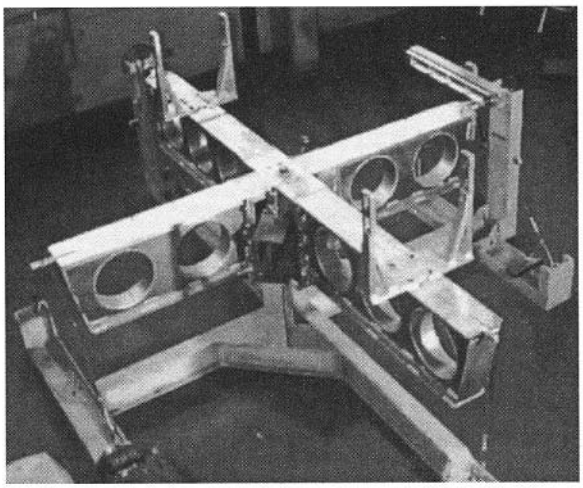

Fig. 7 Mechanism for measuring inertia tensor of large mechanical systems

hence $\hat{\sigma}_1$ and errors increased. As in the first test, the dimensions of the inertia ellipsoid were identified with good accuracy.

Table 3 compares the accuracy of the proposed method with those of other methods (Conti and Bretl, 1989; Pandit and Hu, 1994) and shows lower errors for the proposed method.

The second mechanism is shown in Fig. 7. It was developed with the aim of measuring the inertia tensor of large mechanical systems (mass range: 50–200 kg, maximum dimension about 2 m), like the equipment installed in satellites.

The inertia tensors of several pieces of equipment were identified with good accuracy, because the ratio between residual root mean square $\hat{\sigma}_1$ and the smaller principal moment of inertia was about 2.5 percent.

7 Conclusions

The proposed method for identifying of the inertia tensor of rigid bodies is quite fast, because it requires only one accurate positioning of the specimen and allows the inertia tensor of large bodies to be determined. Since free oscillation around an axis is considered, only an accelerometer and a simple data acquisition system are necessary.

Two prototype mechanisms were built and tested. Experimental results show that the principal moments of inertia, which are related to the dimensions of the inertia ellipsoid, were identified with good accuracy in every condition.

Future development of this research will be identification of center of mass coordinates by means of a similar approach.

Acknowledgments

The authors are grateful to Prof. V. Cossalter for his advice and encouragement during the preparation of this paper. Mrs. G. Walton corrected the English text.

References

Buyanov, E. V., 1991, "Device for Measuring the Inertia Tensor of a Rigid Body," *Measurement Techniques,* Vol. 34, No. 6, pp. 585–589.

Conti, P., and Bretl, J., 1989, "Mount Stiffnesses and Inertia Properties from Modal Test Data," ASME *Journal of Vibration, Acoustics, Stress and Reliability in Design,* Vol. 111, pp. 134–138.

Cossalter, V., Da Lio, M., Lot, R., and Fabbri, L., 1998, "A General Method for the Evaluation of Vehicle Manoeuvrability with Special Emphasis on Motorcycles," *Vehicle System Dynamics,* to appear.

Durisek, N. J., Heydinger, G. J., Chrstos, J. P., and Guenther, D. A., 1997, "Land Vehicle Roll/Yaw Product of Inertia Measurement," ASME JOURNAL OF DYNAMIC SYSTEMS, MEASUREMENT, AND CONTROL, Vol. 119, pp. 212–216.

Fregolent, A., Sestieri, A., and Falzetti, M., 1992, "Identification of Rigid Body Inertia Properties from Experimental Frequency Response," *Proceedings, 10th International Modal Analysis Conference,* San Diego, CA, Vol. 1, pp. 219–225.

Gentile, A., Mangialardi, L., Mantriota, G., and Trentadue, A., 1995, "Measurement of the Inertia Tensor: An Experimental Proposal," *Measurement,* Vol. 16, pp. 241–254.

Gupta, V. K., 1973, "Kinematic Analysis of Plane and Spatial Mechanisms," ASME *Journal of Engineering for Industry,* Vol. 95, pp. 481–486.

Pandit, S., Hu, Z. Q., and Yao, Y. X., 1992, "Experimental Technique for Accurate Determination of Rigid Body Characteristics," *Proceedings, 10th International Modal Analysis Conference,* San Diego, CA, Vol. 1, pp. 307–311.

Pandit, S., Hu, 1994, "Determination of Rigid Body Characteristics from Time Domain Modal Test Data," *Journal of Sound and Vibration,* Vol. 177(1), pp. 31–41.

Toivola, J., and Nuutila, O., 1993, "Comparison of Three Methods for Determining Rigid Body Inertia Properties from Frequency Response Functions," *Proceedings, 11th International Modal Analysis Conference,* Kissimmee, FL, Vol. 2, pp. 1126–1132.